# Adonis: Neural-enhanced Fine-grained Leaf Wetness Sensing with Efficient mmWave Imaging

Yimeng Liu*, Maolin Gan*, Gen Li, Younsuk Dong, Zhichao Cao
*Michigan State University*
{liuyime2, ganmaoli, ligen1, dongyoun, caozc}@msu.edu

***Abstract*—Predicting Leaf Wetness Duration (LWD) is crucial for plant disease control. However, the lack of standardized techniques to measure LWD precisely hampers accurate prediction. While previous works have explored various methods, they fail to quantify the actual water on the leaf, undermining their practical effectiveness and accuracy. This paper presents *Adonis*, an innovative approach using millimeter-wave (mmWave) radar to address the complexities of leaf wetness detection. It introduces a new metric, Leaf Wetness Level (LWL), for measuring leaf surface water. We employ advanced signal processing on mmWave signals to extract more wetness-related features in dynamic environments. Furthermore, we develop a Contrastive Learning Feature Extraction model to precisely capture wetness features and design a calibration process for the inference stage to detect LWLs accurately in real-world fields. Using a frequency-modulated continuous-wave (FMCW) radar within the 77 to 81 GHz band, *Adonis* is meticulously evaluated across various plants. *Adonis* can detect LWLs with the mean absolute error (MAE) of 4.43 in controlled environments and 6.49 in real farm conditions. The performance significantly surpasses traditional Leaf Wetness Sensors, which have an MAE of 11.84 indoors and 14.32 in field conditions. These findings have substantial implications for enhancing disease prediction and crop management.**

## I. Introduction

Food crises are becoming increasingly severe worldwide, with nearly 282 million people in 59 countries facing acute food insecurity in 2023 [1]. The rise in plant disease outbreaks further threatens food security and negatively affects the development of agriculture [2]. Therefore, effective disease control is essential to improve agricultural productivity and ensure sustainability [3]. Leaf Wetness Duration (LWD), which signifies the period of free water presence on the surface of the leaves, directly influences the spread of plant disease [4]. Accurately predicting LWD plays a vital role in disease control and early prevention [5], as it provides better insights into the drying process and disease risk for precise interventions [5], [6]. Recent studies have shown that being attentive to LWD can significantly protect the yields of crops such as apples, corn, and onions [7]–[9].

Currently, researchers have proposed a variety of methods to predict and detect leaf wetness, including LWD modeling [10]–[13], RGB cameras [14], Leaf Wetness Sensors (LWSs) [15], [16] and millimeter-wave (mmWave) radar based approach [17], [18]. However, these approaches exhibit inherent limitations when predicting LWD in real-world scenarios.

* Co-primary Authors.

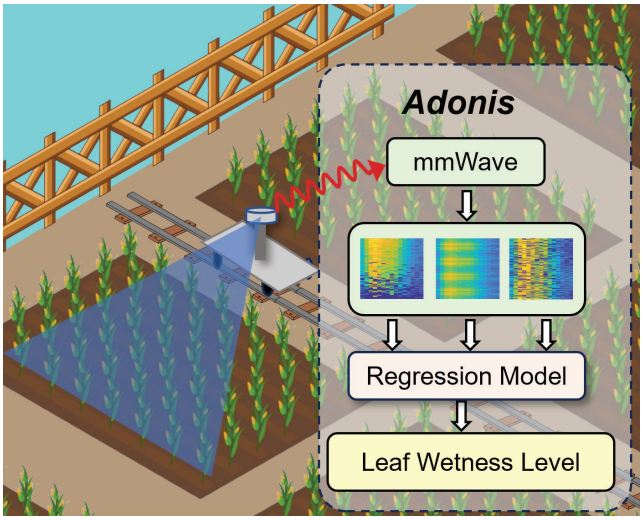


Fig. 1: Leaf Wetness Levels detection with *Adonis*.

**1) Low Accuracy:** Although modeling-based techniques can estimate LWD using various meteorological information, they are sensitive to the quality of environmental data [19], making them not applicable for obtaining accurate results in real farm conditions. The accuracy of systems that use RGB cameras is highly dependent on lighting conditions [20], highly limiting their effective operating times. In addition, LWSs that use synthetic leaves differ from real leaves in size, shape, and material, leading to discrepancies between the detected wetness and actual results [21].

**2) Low Precision:** Current methods lack precision in predicting LWD since they do not adequately reflect the wetness level. For example, systems based on RGB cameras and mmWave radar treat wetness detection as a binary classification problem (wet or dry) without quantifying the water amount. Such binary approaches fail to precisely capture the nuanced changes in leaf wetness over time, which is crucial for LWD prediction.

**3) High System Overhead:** Due to their cumbersome and complex designs, these methods result in significant system overhead from deployment and maintenance. For example, ensuring LWD modeling works properly requires deploying numerous sensors to collect various climate variable data, which inevitably incurs substantial costs [22]. Since each LWS

TABLE I: Methods Comparison for Leaf Wetness Detection.

| Method | Accuracy | Precision | System Overhead |
|---|---|---|---|
| LWD modeling [10]–[13] | Low | High | High |
| RGB camera [14] | Low | Low | Low |
| Leaf Wetness Sensor [15] | Low | High | High |
| mmLeaf [17] | High | Low | High |
| Hydra [18] | High | Low | High |
| ***Adonis*** | **High** | **High** | **Low** |

can only be placed in one location and there is no consensus on the spatial scale it represents [19], deploying and calibrating them over a large area is particularly challenging. Moreover, although mmLeaf can employ synthetic aperture radar (SAR) technology for fine-grained imaging of plants, its sampling efficiency is so low that the time cost of obtaining a single scan result is considerable, which can take up to six minutes [17].

As shown in Table I, previous methods have significant limitations on precisely monitoring leaf wetness changes. Therefore, developing a system that can monitor leaf wetness with high precision and accuracy in complex agricultural environments is critical while maintaining low system overhead.

This paper proposes *Adonis*, a novel mmWave-based system to facilitate accurate leaf wetness monitoring. We introduce Leaf Wetness Level as a quantitative metric detailed in Section II-A to measure the amount of water on the leaf surfaces. We used a high-resolution mmWave radar to sense subtle changes in wetness, as shown in Fig. 1. Since mmWave electromagnetic signals are sensitive to surface texture variations, they can demonstrate different reflection strengths. The reflected signals are enhanced with Fast Fourier Transformation to extract multi-dimensional signal features that are fine-grained and environmentally resilient, enabling precise leaf wetness monitoring even in complex real-world environments. The multi-dimensional signal features are fed into a neural network-based regression model, which performs feature extraction to distinguish between different wetness levels accurately.

*Adonis* outperforms previous systems regarding environmental robustness, accurate LWL detection, and low system overhead design.

However, several challenges must be addressed in developing *Adonis*:

1) **Environmental Noise Mitigation:** The real farm environment presents a significant challenge due to its dynamic and complex nature. Environmental factors such as wind can introduce variations in noise, which can significantly affect the detection of wetness levels. Our solution involves advanced signal processing algorithms to generate 2D signal maps incorporating leaf movement, position, surface texture, information, and signal strength. Combining these data points gives us a robust representation of leaf surface changes that are resilient to environmental variations. This ensures consistent data collection and reliable leaf wetness detection.
2) **Leaf Wetness Levels Regression Model:** Extracting water features from complex signal maps is challenging. Additionally, as defined in Section II-A, LWL is a relative value dependent on complete dryness and saturated wetness, making it challenging to determine LWLs directly from a single wetness feature. To address this, *Adonis* incorporates an innovative regression model to capture and determine the correlations between wetness features. Based on observations from Section II-C, we perform feature extraction by combining contrastive learning with a Convolutional Neural Network (CNN), as shown in Section III-C. Such extraction compares data from the same plant and position with different water amounts, isolating wetness variations from environmental changes for enhanced accuracy. We also include a Wetness Extraction Layer, detailed in Section III-D, which combines baseline saturated wetness and complete dryness to extract LWL-related features accurately.
3) **Model Calibration:** We directly exploit the signals transmitted and reflected by the mmWave radar for detection. Still, a single mmWave sensing result is easily affected by environmental changes, thereby affecting the system's effectiveness across different environments. To address this issue, we design a calibration process with small overheads in the inference stage, applied when scanning different plants or adjusting the radar-plant distance, as detailed in Section III-F. This process involves refining the regression model using a small number of extreme values, including saturated wetness and complete dryness, to ensure system efficiency and enhance its accuracy and reliability.

We implement *Adonis* using a commercial off-the-shelf (COTS) mmWave radar. We evaluate various plant types, sizes, densities, and environmental conditions. Extensive testing of *Adonis* demonstrates its excellent performance across diverse settings. In controlled indoor environments, *Adonis* achieves the mean absolute error (MAE) of $4.43$. In the real farm with different crops and environmental conditions, *Adonis* maintains the MAE of 6.47. In contrast, traditional Leaf Wetness Sensors achieve an MAE of 11.84 indoors and 14.32 in real-field conditions. Despite these dynamic conditions, *Adonis* consistently outperforms existing methods, highlighting its robustness and precision. This is a significant advancement in precision agriculture and plant health monitoring.

The contributions of this paper can be summarized as follows:

- To the best of our knowledge, *Adonis* is the first contactless sensing system specifically designed to measure the amount of water on a leaf, and Leaf Wetness Level (LWL) is the first metric that quantitatively represents leaf wetness.
- We use reflected mmWave signals with signal processing algorithms to create signal feature maps incorporating leaf movement, position, and surface texture. Our model integrates contrastive learning to improve feature extraction based on signal characteristics. This approach

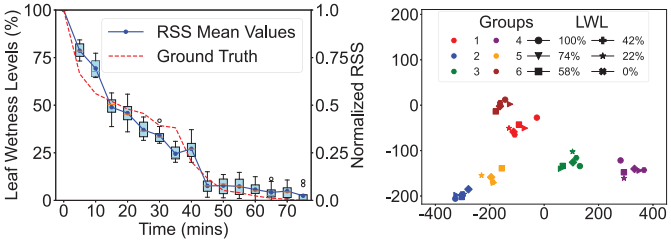


(a) RSS vs Leaf Wetness (b) Received Signal Feature

Fig. 2: Received Signal Feature. RSS has a strong relationship with LWL. The signal shows less distinguishable features among the same LWL.

effectively addresses challenges in distinguishing wetness features from environmental noise, significantly improving the precision and reliability of LWL detection under various conditions.

- The system demonstrates robust performance across different plant types and complex real-field conditions. It achieves the MAE of 4.43 indoors with various plants. Under real-field conditions, it maintains the MAE of 6.49. The traditional Leaf Wetness Sensors show an MAE of 11.84 indoors and 14.32 in real field conditions. This showcases the system's adaptability and effectiveness in varied environmental settings.

## II. Preliminary and Empirical Study

This section introduces LWL as a metric for quantifying leaf wetness. We examine approaches that leverage mmWave technology for LWL detection and review previous efforts to enhance precision.

### A. Leaf Wetness Level

Accurately predicting LWD is crucial for effective plant disease management. It relies heavily on knowing the exact amount of water on the leaf surface, as discussed in Section I. However, no metric exists to accurately evaluate this. To address this gap, we introduce LWL, a new metric that quantitatively represents leaf wetness. LWL is expressed as a continuous variable that varies from $0\%$ to $100\%$. For the $0\%$ represents completely dry which is the plant in a well-ventilated environment at a stable temperature and humidity until no visible droplets remain on the leaf surface indicating it is completely dry. The $100\%$ represents spraying water on the leaf until its surface is fully coated with visible droplets and remains stable, maximally saturated, indicating saturated wetness. The scale between these points is divided into equal increments to represent varying degrees of moisture. For example, a reading of $50\%$ signifies that the leaf is halfway between completely dry and fully saturated. This detailed and accurate measurement of leaf wetness is essential for monitoring drying processes and predicting plant diseases.

### B. mmWave-based Leaf Wetness Sensing

As stated in the previous work for mmWave measurements [17], [18], [23], [24], different materials exhibit varying permittivity and reflect mmWave signals distinctively. Furthermore, the high-frequency bandwidths of the mmWave radar make it sensitive to minor environmental changes [25]. This sensitivity allows it to detect minute variations in the water amount on the leaf. Therefore, mmWave radar is ideal for precise and reliable LWL detection.

In our experiments, the plant is placed approximately 200 mm from the radar in a stationary room with a fixed temperature and no wind. We monitor the transition from saturated wetness to completely dry conditions, sampling with the mmWave and ground truth every 5 minutes over 75 minutes, repeating the process ten times. We apply Range Fast Fourier Transformation for the received signal to extract Received Signal Strength (RSS) based on the plant's position. At the same time, a moisture meter provides ground truth measurements, as discussed in Section IV-B. We normalize the RSS and the ground truth value to a scale of 0-100. As shown in Fig. 2a, we utilize a boxplot to illustrate the normalized RSS distribution at different times. The blue line indicates the trend of the mean normalized RSS value, and the red dotted line shows the ground truth of the change in LWLs. A strong correlation is observed between the normalized RSS and the wetness level; the RSS decreases as the LWL decreases. This observation highlights the potential of using the mmWave reflection intensity to detect changes in LWLs.

### C. mm-Wave-based Received Signal Feature

Directly using RSS has a notable limitation. The short wavelength of the radar would make it more sensitive to environmental changes [23], [26]. mmLeaf [17], and Hydra [18], which uses Synthetic Aperture Radar-Multiple-Input Multiple-Output (SAR-MIMO), need to move the radar to simulate a large aperture that will make the RSS unstable. Only high-resolution imaging of plants with detailed spatial features can not extract accurate and precision LWL information.

We conduct a feature analysis of the received signal to address this limitation and identify crucial elements for building an effective model. We randomly select samples from the entire dataset with varying LWLs and use Principal Component Analysis (PCA) to extract features from the received signals, analyzing the relationships between different plants. Our crucial observation, illustrated in Fig. 2b, shows that samples collected from the same plant in the same location, marked in the same color, exhibit a much stronger relationship. Conversely, samples with the same LWLs, represented by the same marker, revealed few similar features. This finding underscores the challenge faced by traditional feature extraction and regression methods, which struggle to achieve precise results due to the low similarity among samples with similar LWLs. Therefore, it is necessary to design an innovative method to extract valuable features that provide accurate values.

Based on this observation, we define a group as samples collected from the same plant and location but with varying

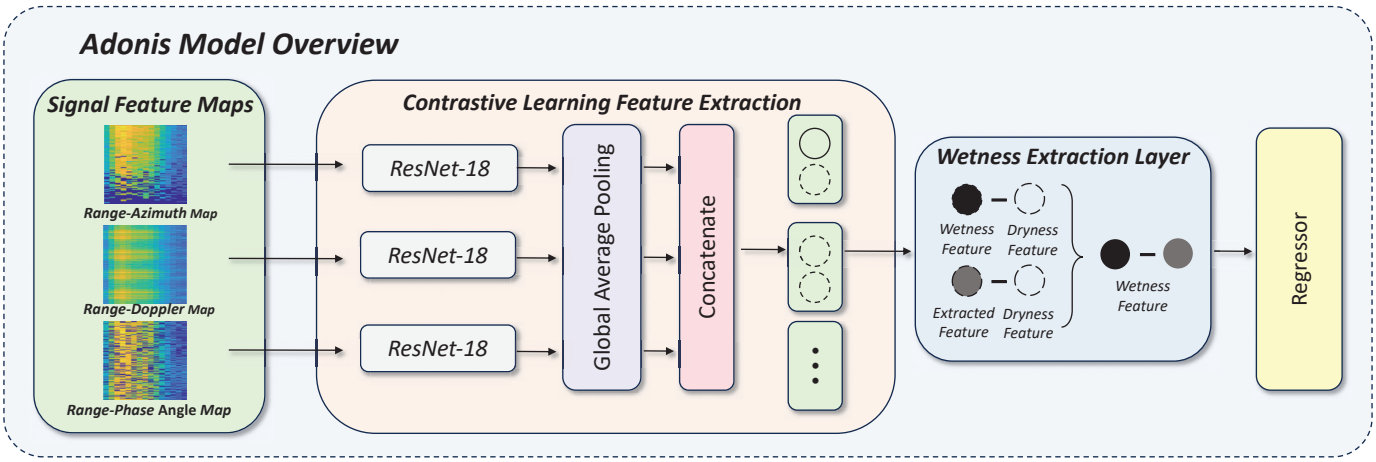


Fig. 3: *Adonis* Model Overview: The *Adonis* model design includes three main procedures: Signal Feature Maps, Contrastive Learning Feature Extraction, and Wetness Extraction Layer.

LWLs. This grouping leverages plant-specific consistency. It helps us to design *Adonis* by extracting and comparing the wetness feature within a group to achieve high precision and accurate detection of LWL.

## III. System Design

### A. Overall Architecture

We present *Adonis*, an advanced leaf wetness sensing system. *Adonis* integrates mmWave technology to facilitate the detection of various LWLs. Its precise and durable architecture, illustrated in Fig. 3, comprises key components: mmWave radar, signal processing (Section III-B), the Contrastive Learning Feature Extraction (Section III-C), Wetness Extraction layer (Section III-D), Model Training (Section III-E) and Calibration (Section III-F). In the following, we describe these components in detail.

### B. mmWave Signal Processing

As stated in [23], [26], mmWave RSS is susceptible to environmental changes. This sensitivity poses a significant challenge: the relationship between RSS and LWLs can be substantially degraded in dynamic environments. This variability complicates accurate detection and requires robust signal processing techniques to maintain reliability and precision under various conditions.

We use Fast Fourier Transformation (FFT) to address these challenges and extract high-dimensional feature maps that preserve RSS across different environments while capturing more wetness-related changes.

To handle dynamic environmental effects, *Adonis* uses a Range-Doppler (RD) map to extract movement information. This technique leverages the Doppler effect to determine the relative velocity of the target leaves, ensuring that the relationship between the RSS and wetness level changes is maintained in different conditions. The RD map is computed in two stages: transforming the IQ data from the time domain to the range domain and from the range domain to the Doppler domain. The range-domain transformation is defined as:

$$R(m,n) = \sum_{k=1}^{K} \mathrm{IQ}(m,k) \cdot e^{-j2\pi \frac{kn}{N}} \tag{1}$$

where $\mathrm{IQ}(m,k)$ represents the IQ data for chirp index $m$ and sample index $k$. The term $e^{-j2\pi \frac{kn}{N}}$ applies the Fourier Transform to convert the time-domain samples into range-domain bins, with $N$ being the number of points in the range FFT.

The Doppler-domain transformation is then performed as:

$$RD(m,n) = 20 \cdot \log_{10}\left(\left|\sum_{p=1}^{P} R(p,n) \cdot e^{-j2\pi \frac{mp}{M}}\right|\right) \tag{2}$$

where $RD(m,n)$ represents the Range-Doppler feature map, with $m$ being the Doppler bin index and $n$ the range bin index. Here, $R(p,n)$ is the range-domain data obtained from the first transformation for chirp $p$ and range bin $n$. The term $e^{-j2\pi \frac{mp}{M}}$ applies the Fourier Transform to convert the chirp-domain data into Doppler-domain data, resolving the velocity information. $M$ is the number of points in the Doppler FFT. The magnitude of the resulting complex value is then taken and expressed in decibels (dB) using the $20 \cdot \log_{10}$ operation. The Example of the Range-Doppler map is shown in Fig. 4a.

The Range-Azimuth (RA) mapping precisely locates the target plant within the radar's field of view by integrating azimuth data, ensuring consistent signal readings despite plant position changes or environmental conditions. An example of the RA map is shown in Fig. 4b. This map is derived using the range-domain transformation, as detailed in Eq. 1. Subsequently, the azimuth-domain transformation is performed as follows:

$$RA(m,\theta) = \sum_{n=1}^{N} R_n(m,k) \cdot \delta\left(\theta - \sin^{-1}\left(\frac{\Delta\phi_{mn}\lambda}{2\pi d}\right)\right) \tag{3}$$

where $RA(m,\theta)$ represents the RA feature map, where $m$ is the range bin and $\theta$ is the estimated angle of arrival

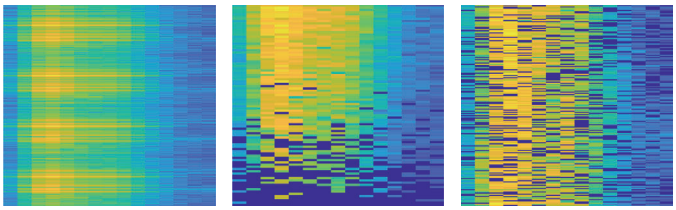

(a) RD Map (b) RA Map (c) RPA Map

Fig. 4: Example of signal feature map processed from the received IQ data.

(AoA). The term $R_n(m,k)$ is the range-transformed IQ data from antenna $n$ calculated in Eq. 1. The Dirac delta function $\delta\left(\theta - \sin^{-1}\left(\frac{\Delta\phi_{mn}\lambda}{2\pi d}\right)\right)$ accumulates signal intensities corresponding to the angles calculated using the phase differences $\Delta\phi_{mn}$, the wavelength $\lambda$, and the antenna separation $d$. $N$ is the number of antennas.

In addition, phase angle changes provide crucial information about the variations in leaf surface texture, which fluctuate with the amount of water present. The dielectric constant and conductivity of a medium affect the propagation speed of the wave, causing changes in the phase angle [23]. This relationship is effectively captured using a Range-Phase Angle (RPA) map, correlating these texture variations with changes in wetness level to enhance detection accuracy. The RPA map is derived using the range-domain transformation, as detailed in Eq. 1. Following this, the Phase Angle transformation is performed as follows:

$$RPA(m,\phi) = \sum_{k=1}^{K} \left| \sum_{n=1}^{N} R_n(m,k) \right| \cdot \delta\left(\phi - \frac{\phi_{mk} \cdot 180}{\pi}\right) \quad (4)$$

where $RPA(m,\phi)$ represents the Range-Phase Angle feature map for range bin $m$ and phase angle $\phi$. The term $R_n(m,k)$ is the range-transformed IQ data from antenna $n$ calculated in Eq. 1. The magnitude $\left|\sum_{n=1}^{N} R_n(m,k)\right|$ is calculated by summing the contributions from all antennas. The Dirac delta function $\delta\left(\phi - \frac{\phi_{mk}\cdot 180}{\pi}\right)$ accumulates signal intensities corresponding to the phase angles calculated using $\phi_{mk}$ (the phase of the signal for range bin $m$ and sample index $k$), converted to degrees. $N$ is the number of antennas. An example of the calculation results for the Range-Phase Angle map is shown in Fig. 4c.

By integrating these signal processing techniques, *Adonis* maintains high precision and environmental resilience, even under varying conditions.

### C. Contrastive Learning Feature Extraction

The PCA results of Section II-B reveal that features are similar within the same plant and position but less consistent within the same LWLs. Traditional feature extraction methods aim to identify consistent features in samples to achieve accurate results, but the lack of unique features complicates precise detection. Additionally, mmWave signals from a single scan are more susceptible to distribution issues, resulting in a low signal-to-noise ratio (SNR), complicating the precise detection of LWLs. This requires designing an innovative model to extract wetness features and create a high-precision regression model.

Contrastive learning creates robust representations by learning embeddings in which the extracted features from similar pairs are closer together, and those from different pairs are farther apart. Initially applied in face recognition [27] and signature verification [28].

We utilize contrastive learning to address the challenge of precise LWL detection. We define a group as samples from the same radar and plant setup but with different LWLs as detailed in Section II-C. This technique enhances intragroup similarity and intergroup distinctiveness, enabling the regression model to focus on the wetness feature changes within a group and improving detection accuracy. Furthermore, concentrating on each group allows the model to filter out noise, leading to more precise and reliable wetness detection.

We use ResNet-18 [29] to extract the feature from each signal feature map as introduced in Section III-B to implement contrastive learning. CNNs like ResNet-18 are ideal for analyzing 2D images because they can capture spatial hierarchies and local patterns. ResNet-18's residual layers allow deeper network architectures without encountering the vanishing gradient problem. This enables the network to learn complex and abstract features by preserving information across multiple layers.

Due to the different information presented by the three signal feature maps, we apply three separate ResNet-18 models to extract features. Additionally, we incorporate a Global Average Pooling (GAP) layer [30]. This layer calculates the spatial mean of feature maps from the final convolution layer, streamlining data complexity while preserving essential features without adding new trainable parameters. We then concatenate the extracted features to prepare for regression.

We will first pre-train the feature extraction model. The feature maps within the same group are labeled 1, and those from different groups are labeled 0. To measure the similarity between these feature maps, we calculate the $L^2$ distance, defined as

$$d_{ij} = \sqrt{\sum_{k} (f_i^k - f_j^k)^2} \quad (5)$$

where $f_i$ and $f_j$ are the feature vectors of samples $i$ and $j$, respectively.

The contrastive loss function we used is formulated as follows:

$$\mathcal{CL} = \frac{1}{N} \sum_{i,j} [y_{ij} \cdot d_{ij}^2 + (1 - y_{ij}) \cdot \max(0, m - d_{ij})^2] \quad (6)$$

In this loss function, $y_{ij}$ is a binary label that indicates if the pair $(i,j)$ is similar or different, and $m$ is a margin parameter that sets the minimum distance for dissimilar pairs. The loss function penalizes similar pairs far apart and dissimilar pairs closer than the margin, driving the network to position the

same group together and different groups apart. Including a margin ensures that dissimilar pairs maintain a minimum separation, reducing noise influence and enhancing overall model performance.

### D. Wetness Extraction Layer

To accurately determine LWL, we employ a wetness extraction layer. This layer is essential for standardizing LWL measurements and removing noise. The wetness extraction layer is defined as:

$$LWL = (W - D) - (F - D) \tag{7}$$

where $W$ represents the wetness baseline (100% wetness), $D$ represents the dryness baseline (0% wetness), and $F$ is the current extracted feature. Calculating the difference between the wetness and dryness baselines ($W - D$) allows us to establish a net wetness value that aligns with the defined LWL boundaries. By subtracting the dryness feature ($D$) from the extracted feature ($F$), we ensure the model focuses on the wetness feature and mitigates environmental noise. Finally, subtracting this result from the net wetness aligns the measurement with the definition of LWL, ensuring that the final values accurately reflect the relative amount of water on the leaf.

### E. Model Training

To train our model, we use the mean squared error (MSE) as the loss function and mean absolute error as the evaluation metric. MSE measures the average of the squared differences between predicted and actual LWLs, which is particularly effective for regression tasks because it significantly penalizes more significant errors. This encourages the model to make precise predictions by focusing on reducing substantial deviations. We use MAE to calculate the average absolute differences between the predicted and actual values for performance evaluation. MAE offers a straightforward interpretation of prediction accuracy and is less sensitive to outliers than MSE, providing a precise measure of the average prediction error. The MSE and MAE is defined as:

$$\text{MSE} = \frac{1}{n}\sum_{i=1}^{n}(y_i - \hat{y}_i)^2 \tag{8}$$

$$\text{MAE} = \frac{1}{n}\sum_{i=1}^{n}|y_i - \hat{y}_i| \tag{9}$$

where $y_i$ represents the actual values, $\hat{y}_i$ represents the predicted values, and $n$ is the number of samples.

### F. Calibration

Based on Section II-C, our scan method is susceptible to subtle environmental changes. We implement a calibration stage with a small system overhead to ensure prediction accuracy. Calibration is necessary before each detection, mainly when dealing with different plants and changes in the radar's relative position.

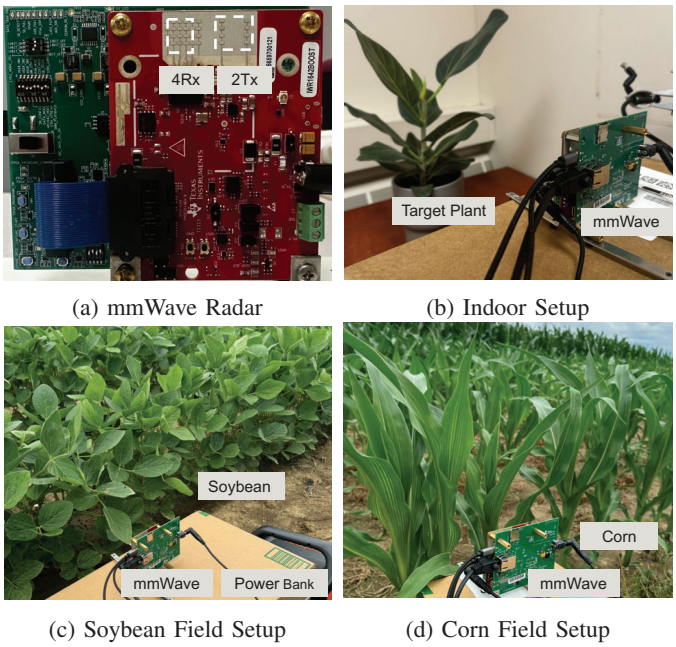


(a) mmWave Radar (b) Indoor Setup

(c) Soybean Field Setup (d) Corn Field Setup

Fig. 5: *Adonis* setup with mmWave Radar: Deployment in various scenarios, including indoor, soybean, and corn fields.

During the inference stage, we first collect data from extreme values, representing complete dryness and saturated wetness. We use the extreme data to refine the entire model. This process includes refining the Contrastive Learning Feature Extraction to maintain intragroup similarity and enhance intergroup dissimilarity, ensuring precise feature extraction. Furthermore, this calibration refines the regressor to detect LWLs accurately. By systematically calibrating the model, we ensure its robustness and reliability across various environmental conditions, improving its overall performance.

## IV. Implementation

### A. System Implementation

We develop a prototype for *Adonis*, as shown in Fig. 5a, using the Texas Instruments (TI) IWR1642 mmWave radar [31], which operates in the 77 to 81 GHz frequency range. The radar features four horizontal receiver antennas, providing excellent azimuth angle resolution. To complement the radar, we use a DCA 1000EVM [32] for initial signal collection and processing, which sets the stage for detailed analysis.

### B. Ground Truth

Due to the lack of a specialized sensor to track LWLs accurately, we designed an innovative method to establish a reliable ground truth. We employ a commercial moisture meter from General Tools [33], commonly used to measure wetness levels on wood surfaces. This device measures the electrical resistance between two pins, as illustrated in Fig. 6. Although not specifically designed to detect leaf surface wetness, it serves our needs. By gently pressing the moisture meter pins onto the leaf surface, we can detect variations

(a) Dry Leaf (b) Wet Leaf

Fig. 6: Moisture Meter Utilized for Ground Truth.

in electrical resistance corresponding to the leaf's moisture content. We utilized the change in readings to measure the LWLs. Initially, we calibrated the moisture meter by setting the baseline readings for complete dryness at 0% The readings are then normalized based on these baselines to determine the LWLs.

### C. Baseline

We use commercial Leaf Wetness Sensors in our experimental setup, namely the PHYTOS 31 model [15], which measures water changes in surface according to electrical resistance. However, the metal parts of the sensor caused more backscatter, which could have compromised the mmWave's precision. To compromise this problem, we employ a plant of comparable size in the same habitat as the species under observation. To simulate leaf locations, we arrange three sensors in an equal distribution throughout the plant's foliage. We calibrate the readings by setting baselines for complete saturation and total dryness. We normalize the other readings based on these baselines to determine the LWLs.

### D. Data Collection

Our experimental setup gathers data from six diverse plant types, focusing on plant size, leaf size, and leaf density variations. Data collection occurs in both controlled indoor environments and real field environments. We include a stable environment shown in Fig. 5b and a simulated wind environment for the indoor setup using a fan. We also conducted in-situ experiments in two fields totaling 3.67 acres, planted with soybeans shown in Fig. 5c and corn in Fig. 5d. The distance between the closest point of the plant and the radar ranged from 200 to 400 mm, with an extracted range of 100 to 500 mm to capture comprehensive signal feature maps, as detailed in Section III-B. Each data collection group involves spraying plants. It treats them until they reach saturated wetness and then allows them to dry completely, treating each plant's entire wet-to-dry process as a group, as detailed in Section II-C. Each group receives 6 to 12 samples based on temperature and evaporation rates. The process collects 508 groups with 4849 samples, including 358 groups and 3330 samples from indoor environments and 180 groups and 1789 samples from outdoor environments, ensuring robust data for analyzing LWLs under different conditions.

### E. System Evaluation

To evaluate the precision of our models, we employ a 5-fold cross-validation, iterated 10 times across different datasets. This rigorous approach minimizes variability and bias from the diverse dataset, ensuring that our performance metrics accurately reflect the model's capabilities under various conditions. To simulate the inference stage during the evaluation, we calibrate the model according to the process described in Section III-F. This calibration step is crucial for aligning the model's predictions with real-world conditions, thereby enhancing the reliability of our results.

## V. Evaluation

### A. Overall Performance

In our evaluation of *Adonis*, we focus on its precision in discerning various LWLs. Our system uses an extensive dataset to demonstrate exceptional accuracy, achieving the MAE of $4.43 \pm 0.57$. Compared, LWSs exhibit a much larger MAE of $11.27 \pm 2.08$. As in the comparison shown in Fig. 7a, these results indicate a significant difference between *Adonis* and traditional sensors compared to the ground truth. LWSs show greater error and variability in the detection of LWLs. This discrepancy is primarily due to the sensor not measuring the leaf surface; different sensor placements can lead to inconsistent results. Even different sensor places in the same plant can have different readings, making them less reliable and accurate compared to *Adonis*.

### B. System Overhead Analysis

Compared to the mmLeaf system [17], which uses mmWave radar with MIMO-SAR techniques for plant imaging, *Adonis* shows significant improvements in efficiency and practicality. We conduct 50 tests to evaluate the elapsed time for each system. While mmLeaf requires extensive processing time, typically exceeding 455.58 seconds per scan, and necessitates scanning the entire area, *Adonis* achieves accurate measurements in under 8.21 seconds per scan by only needing a single scan. Furthermore, LWS [15] can only be deployed in one specific location, and modeling LWD [10]–[13] requires numerous weather sensors, making widespread deployment and calibration challenging. This system overhead is crucial for large-scale agricultural applications. The ease of deployment and rapid data collection of *Adonis* allows frequent scanning of multiple plants, improving leaf wetness changes monitoring and allowing farmers to make timely decisions based on wetness trends.

### C. Calibration Analysis

Based on Section III-B, mmWave is highly sensitive to subtle changes in dynamic environments, necessitating calibration as designed in Section III-F to accommodate its instability. We train the model using the same dataset and validate the results with and without calibration. As shown in Fig. 7b, the

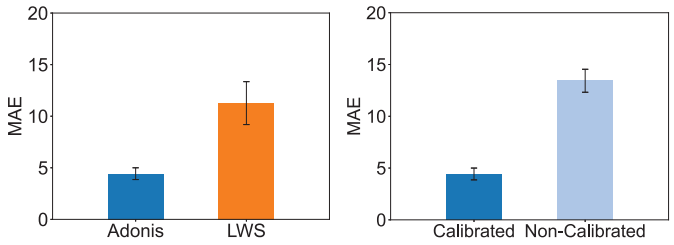


(a) LWLs Detection (b) Calibration Performance

Fig. 7: *Adonis* Precision and Calibration Performance

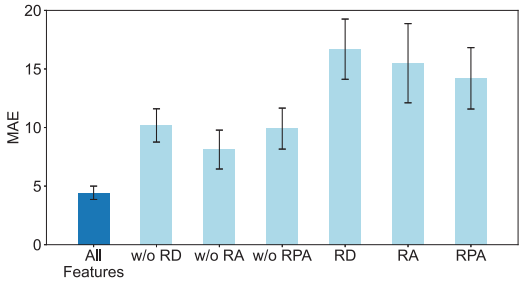


Fig. 8: Ablation Study Performance for Signal Processing

model without calibration significantly increases the MAE to $13.43 \pm 1.1$, while the calibration improved precision, reducing the MAE to $4.43 \pm 0.57$. This demonstrates the critical role of calibration in improving the accuracy and reliability of the model in varying environmental conditions.

### *D. Signal Processing Evaluation*

In Section III-B, we detail three signal processing techniques utilized in *Adonis*: Range-Doppler, Range-Phase Angle, and Range-Azimuth mappings. Each method is essential for accurately detecting LWLs by capturing unique aspects of the mmWave signal. To assess the effectiveness of each feature map, we conduct an ablation study [34] that systematically removes one or two maps and tests the remaining combinations. The result is shown in Fig. 8. When using all three signal processing techniques, the system achieves the MAE of $4.43 \pm 0.57$. Removing the Range-Doppler, Range-Azimuth, and Range-Phase Angle techniques result in higher MAEs of $10.18 \pm 1.66, 8.12 \pm 1.42$, and $9.91 \pm 1.75$, respectively. When only one feature map is retained, leaving either Range-Doppler, Range-Azimuth, or Range-Phase Angle, the MAEs increase to $16.68 \pm 2.57$, $15.49 \pm 3.38$, and $14.20 \pm 2.62$, respectively. These results confirm that each signal processing technique captures distinct and complementary information, underscoring the necessity of all three methods for robust and accurate LWL detection.

### *E. Application in Different Environments*

In evaluating the performance of *Adonis* under various environmental conditions, we focus on different plant sizes and leaf sizes, wind/no wind scenarios, and indoor/real farm settings.

We evaluate *Adonis* on plants with large, sparse, and small, dense leaves, the two most common plant patterns. Research indicates that large leaves are prevalent in warm, humid regions to maximize photosynthesis, while smaller leaves are typical in cold, dry areas for better water use efficiency [35]. This comprehensive test ensures that *Adonis* performs well in all major plant categories. Our system consistently performs well in all types of plants shown in Fig. 9a, achieving the MAE of $4.14 \pm 0.52$ for plants with large sparsity leaves and $3.97 \pm 0.71$ for small dense leaves, demonstrating its adaptability and accuracy regardless of plant size and leaf characteristics. Meanwhile, we test with the LWS for large, sparse, and small, dense leaves to obtain the MAE for $10.52 \pm 1.16, 11.63 \pm 2.12$.

As stated in Section II-C, mmWave signals are easily affected by subtle changes, especially wind in outdoor environments. We focus on moderate wind conditions and exclude extreme scenarios, as high wind speeds rapidly dry the leaves, rendering them irrelevant for analyzing the wetness drying process. To assess the impact of wind, we conduct experiments in controlled indoor environments with and without fans simulating wind conditions. The system achieves high accuracy without wind with the MAE of $3.05 \pm 0.43$. Under windy conditions, the MAE increases to $5.02 \pm 0.72$, indicating the system's resilience to environmental disturbances. This robustness under windy conditions showcases *Adonis*'s capability to maintain accurate LWLs detection despite external factors. See Figure 9b for a comparison of the results. Additionally, we test with LWSs, obtaining MAEs of $8.63 \pm 2.24$ without wind and $10.72 \pm 3.74$ under windy conditions.

The performance of the *Adonis* system is further evaluated by assessing its accuracy at varying distances from a target plant in an indoor setting. Measurements are taken from the closest point of the plant to the radar. As depicted in Fig. 9c, the system achieves its lowest MAE of 3.98 when the plant was positioned 200mm away. When the distance increases to 300mm and 400mm, the MAE slightly rises to 4.32 and 4.72, respectively. This indicates a trend where increasing distance results in decreased mmWave resolution. These findings suggest that while *Adonis* maintains robust performance over different distances relative to the target.

We also evaluate *Adonis* in both indoor and in-situ settings. Indoor experiments are conducted in controlled environments, while outdoor experiments occur in real fields with corn and soybeans. As shown in Fig. 9d, *Adonis* achieves the MAE of $4.05 \pm 0.63$ indoors and $6.47 \pm 1.02$ outdoors, confirming its reliability and effectiveness in diverse environments. The indoor and outdoor results for the LWS are $11.84 \pm 2.06$ and $14.32 \pm 5.28$, respectively. These results demonstrate that *Adonis* can provide accurate LWL measurements for effective disease prediction and agricultural management in real-world scenarios.

## VI. RELATED WORK

**Leaf Water Content.** Accurate leaf water content (LWC) measurement is crucial for agricultural management. LWC,

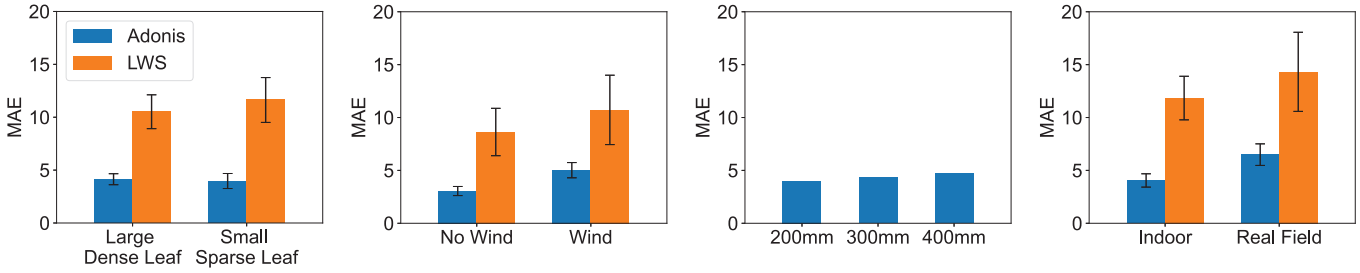


(a) Different Distance (b) Wind Scenario (c) Plant Distance (d) Real Field Scenario

Fig. 9: Performance for *Adonis* Application in Various Scenario.

defined as the amount of water in leaf tissue, is typically measured as a percentage of the leaf's fresh weight and is closely related to but distinct from Leaf Wetness Levels (LWLs). Techniques like near-infrared spectroscopy [36] and mmWave technology [37], [38] offer real-time monitoring advantages due to their sensitivity and penetration depth, enabling continuous assessment of leaf moisture levels.

**Real-World Denoising Applications.** Denoising in real-world sensing applications is vital for data accuracy. Deep learning methods, such as autoencoders and generative adversarial networks (GANs), have significantly enhanced signal quality in environmental monitoring and health diagnostics [39]–[44]. These techniques effectively reduce noise, improving the clarity and usability of sensor data collected in noisy environments, which is crucial for precise leaf wetness detection.

**Agriculture Internet of Things.** Integrating the Internet of Things (IoT) and Artificial Intelligence (AI) into agriculture has revolutionized traditional farming practices, creating a powerful AIoT approach to enhance efficiency and decision-making [45]. Sensing in agriculture enables monitoring of soil moisture and macronutrients [46]–[49], providing data for precise resource management and early issue detection. Communication in agriculture faces challenges, such as limited connectivity in remote areas and high energy demands for data transmission. Technologies like LoRa [50]–[54], and satellite [55] address these issues by enabling low-power, long-range communication. They provide reliable data transfer from distributed sensors to centralized systems.

## VII. Conclusion

This paper presents the development, deployment, and comprehensive evaluation of *Adonis*, an advanced system for precise Leaf Wetness Levels detection. We introduce a new metric, Leaf Wetness Level, which accurately quantifies the amount of water on a leaf surface. *Adonis* addresses critical challenges such as environmental denoising, LWL regression modeling, and calibration. We incorporate mmWave signal with three distinct signal processing techniques to explore wetness features in dynamic environments: Range-Doppler, Range-Azimuth, and Range-Phase Angle maps. Extensive experiments conducted under various real-world conditions, including different leaf sizes, densities, and environmental factors, demonstrate that *Adonis* consistently outperforms existing methodologies in accuracy and reliability. It achieves a mean absolute error of 4.43 in controlled settings and maintains an MAE of around 6.49 in real farm environments, whereas traditional Leaf Wetness Sensors have an MAE of 11.84 indoors and 14.32 in real-field conditions. These findings highlight *Adonis*'s robustness and precision in detecting leaf wetness, representing a significant advancement in precision agriculture.

## Acknowledgement

We sincerely thank the anonymous reviewers for their valuable feedback. This work was partially supported by NSF CAREER Award 2338976.

## References

[1] G. N. A. F. Crises and F. S. I. Network. (2024) Global report on food crises (grfc) 2024. Accessed: 2024-07-31. [Online]. Available: https://www.wfp.org/publications/global-report-food-crises-grfc-2024

[2] J. B. Ristaino, P. K. Anderson, D. P. Bebber, K. A. Brauman, N. J. Cunniffe, N. V. Fedoroff, C. Finegold, K. A. Garrett, C. A. Gilligan, C. M. Jones, M. D. Martin, G. K. MacDonald, P. Neenan, A. Records, D. G. Schmale III, L. Tateosian, and Q. Wei, "The persistent threat of emerging plant disease pandemics to global food security," *Proceedings of the National Academy of Sciences*, vol. 118, no. 23, p. e2022239118, 2021.

[3] D. J. Mulla, "Twenty five years of remote sensing in precision agriculture: Key advances and remaining knowledge gaps," *Biosystems Engineering*, vol. 114, pp. 358–371, 4 2013.

[4] T. Rowlandson, M. Gleason, P. Sentelhas, T. Gillespie, C. Thomas, and B. Hornbuckle, "Reconsidering leaf wetness duration determination for plant disease management," *Plant Disease*, vol. 99, pp. 310–319, 2015.

[5] W. Uddin, K. Serlemitsos, and G. Viji, "A temperature and leaf wetness duration-based model for prediction of gray leaf spot of perennial ryegrass turf," *Phytopathology*, 2003.

[6] C. Moragrega and I. Llorente, "Effects of leaf wetness duration, temperature, and host phenological stage on infection of walnut by xanthomonas arboricola pv. juglandis," *Plants*, vol. 12, 8 2023.

[7] M. Launay, O. Zurfluh, F. Huard, S. Buis, G. Bourgeois, J. Caubel, L. Huber, and M. O. Bancal, "Robustness of crop disease response to climate change signal under modeling uncertainties," *Agricultural Systems*, vol. 178, p. 102733, 2 2020.

[8] F. Nabi, S. Jamwal, and K. Padmanbh, "Wireless sensor network in precision farming for forecasting and monitoring of apple disease: a survey," *International Journal of Information Technology*, vol. 14, 2022.

[9] H. Furuya, H. Takanashi, S. I. Fuji, Y. Nagai, and H. Naito, "Modeling infection of spring onion by puccinia allii in response to temperature and leaf wetness," *Phytopathology*, vol. 99, pp. 951–956, 8 2009.

[10] A. Weiss, D. Lukens, J. Norman, and J. Steadman, "Leaf wetness in dry beans under semi-arid conditions," *Agricultural and Forest Meteorology*, vol. 48, no. 1, pp. 149–162, 1989. [Online]. Available: https://www.sciencedirect.com/science/article/pii/0168192389900130

[11] P. C. Sentelhas, A. D. Marta, S. Orlandini, E. A. Santos, T. J. Gillespie, and M. L. Gleason, "Suitability of relative humidity as an estimator of leaf wetness duration," *Agricultural and Forest Meteorology*, vol. 148, pp. 392–400, 3 2008.

[12] S. Zito, T. Castel, Y. Richard, M. Rega, and B. Bois, "Optimization of a leaf wetness duration model," *Agricultural and Forest Meteorology*, vol. 291, p. 108087, 9 2020.

[13] W. Luo, "Simulation and measurement of leaf wetness formation in paddy rice crops," *Agricultural and Forest Meteorology*, vol. 88, pp. 1–14, 1996.

[14] A. Patel, W. S. Lee, N. A. Peres, and C. W. Fraisse, "Strawberry plant wetness detection using computer vision and deep learning," *Smart Agricultural Technology*, vol. 1, p. 100013, 2021.

[15] M. Group. (2021) Phytos 31 manual. METER Group. Accessed: 2024-07-31. [Online]. Available: http://library.metergroup.com/Manuals/20434_PHYTOS31_Manual_Web.pdf

[16] B. H. Nguyen, G. S. Gilbert, and M. Rolandi, "A bio-mimetic leaf wetness sensor from replica molding of leaves," *Advanced Sensor Research*, vol. 2, no. 6, p. 2200033, 2023.

[17] M. Gan, Y. Liu, L. Liu, C. Wu, Y. Dong, H. Zeng, and Z. Cao, "Poster: mmleaf: Versatile leaf wetness detection via mmwave sensing," in *Proceedings of ACM MobiSys*, 2023.

[18] Y. Liu, M. Gan, H. Zeng, L. Li, Y. Dong, and Z. Cao, "Hydra: Accurate multi-modal leaf wetness sensing with mm-wave and camera fusion," in *Proceedings of ACM MobiCom*, 2024.

[19] T. Rowlandson, M. Gleason, P. Sentelhas, T. Gillespie, C. Thomas, and B. Hornbuckle, "Reconsidering leaf wetness duration determination for plant disease management," *Plant disease*, vol. 99, no. 3, pp. 310–319, 2015.

[20] J. Romeo, J. M. Guerrero, M. Montalvo, L. Emmi, M. Guijarro, P. Gonzalez-de Santos, and G. Pajares, "Camera sensor arrangement for crop/weed detection accuracy in agronomic images," *Sensors*, vol. 13, no. 4, pp. 4348–4366, 2013.

[21] A. B. Gama, D. Perondi, M. M. Dewdney, C. W. Fraisse, I. M. Small, and N. A. Peres, "Evaluation of a multi-model approach to estimate leaf wetness duration: an essential input for disease alert systems," *Theoretical and Applied Climatology*, vol. 149, no. 1, pp. 83–99, 2022.

[22] K. Alsafadi, B. Alatrach, S. S. Sammen, and W. Cao, "Prediction of daily leaf wetness duration using multi-step machine learning," *Computers and Electronics in Agriculture*, vol. 224, p. 109131, 2024.

[23] Y. Liang, A. Zhou, H. Zhang, X. Wen, and H. Ma, "Fg-liquid: A contactless fine-grained liquid identifier by pushing the limits of millimeter-wave sensing," *Proc. ACM Interact. Mob. Wearable Ubiquitous Technol.*, vol. 5, no. 3, sep 2021.

[24] A. Kamari, Y. Chae, and P. Pathak, *mmSV: mmWave Vehicular Networking using Street View Imagery in Urban Environments*. New York, NY, USA: Association for Computing Machinery, 2023. [Online]. Available: https://doi.org/10.1145/3570361.3613291

[25] H. Zhang, A. S. Rathore, X. Chen, K. Wang, M. chun Huang, C. Xu, H. Li, Z. Li, M.-C. Huang, and W. Xu, "Cardiacwave: A mmwave-based scheme of non-contact and high-definition heart activity computing," *Computing. Proc. ACM Interact. Mob. Wearable Ubiquitous Technol*, vol. 5, p. 135, 2021. [Online]. Available: https://doi.org/10.1145/3478127

[26] Z. Meng, S. Fu, J. Yan, H. Liang, A. Zhou, S. Zhu, H. Ma, J. Liu, and N. Yang, "Gait recognition for co-existing multiple people using millimeter wave sensing," in *Proceedings of the AAAI*, 2020.

[27] J. Bromley, J. W. Bentz, L. Bottou, I. Guyon, Y. LeCun, C. S. Moore, E. Säckinger, and R. Shah, "Signature verification using a "siamese" time delay neural network," in *Advances in neural information processing systems*, 1994.

[28] S. Chopra, R. Hadsell, and Y. LeCun, "Learning a similarity metric discriminatively, with application to face verification," in *Proceedings of IEEE CVPR*, 2005.

[29] K. He, X. Zhang, S. Ren, and J. Sun, "Deep residual learning for image recognition," in *Proceedings of IEEE CVPR*, 2016.

[30] M. Lin, Q. Chen, and S. Yan, "Network in network," 2014.

[31] Texas Instruments, "Iwr1642," https://www.ti.com/product/IWR1642, 2024, accessed: 2024-07-31.

[32] T. Instruments, "Dca1000evm," https://www.ti.com/tool/DCA1000EVM, 2024, accessed: 2024-07-31.

[33] General Tool, "Moisture meter," https://generaltools.com/digital-tools/moisture-humidity-digital-tools/moisture-meters, accessed: 2024-07-31.

[34] R. Meyes, M. Lu, C. W. de Puiseau, and T. Meisen, "Ablation studies in artificial neural networks," 2019. [Online]. Available: https://arxiv.org/abs/1901.08644

[35] I. J. Wright, N. Dong, V. Maire, I. C. Prentice, M. Westoby, S. Díaz, R. V. Gallagher, B. F. Jacobs, R. Kooyman, E. A. Law, M. R. Leishman, Ülo Niinemets, P. B. Reich, L. Sack, R. Villar, H. Wang, and P. Wilf, "Global climatic drivers of leaf size," *Science*, vol. 357, no. 6354, pp. 917–921, 2017.

[36] E. Hunt and B. N. Rock, "Detection of changes in leaf water content using near- and middle-infrared reflectances," *Remote Sensing of Environment*, vol. 30, no. 1, pp. 43–54, 1989. [Online]. Available: https://www.sciencedirect.com/science/article/pii/0034425789900461

[37] M. Cardamis, H. Jia, H. Qian, W. Chen, Y. Yan, O. Ghannoum, A. Quigley, C. T. Chou, and W. Hu, "Leafeon: Towards accurate, robust and low-cost leaf water content sensing using mmwave radar," 2024. [Online]. Available: https://arxiv.org/abs/2410.03680

[38] J. F. T. Theumer and A. Zajic, "A new mm-wave backscattering method for estimating water content in leaves to minimize demand on water resources," *IEEE Access*, vol. 12, pp. 38 298–38 303, 2024.

[39] D. Jana, J. Patil, S. Herkal, S. Nagarajaiah, and L. Duenas-Osorio, "Cnn and convolutional autoencoder (cae) based real-time sensor fault detection, localization, and correction," *Mechanical Systems and Signal Processing*, vol. 169, p. 108723, 2022.

[40] D. M. Vo, D. M. Nguyen, T. P. Le, and S.-W. Lee, "Hi-gan: A hierarchical generative adversarial network for blind denoising of real photographs," *Information Sciences*, vol. 570, pp. 225–240, 2021.

[41] R. Wang, Y. Liu, and R. Müller, "Detection of passageways in natural foliage using biomimetic sonar," *Bioinspiration & Biomimetics*, vol. 17, no. 5, p. 056009, 2022.

[42] H. Zeng, G. Li, and T. Li, "Pyrosense: 3d posture reconstruction using pyroelectric infrared sensing," *Proceedings of the ACM on Interactive, Mobile, Wearable and Ubiquitous Technologies*, vol. 7, no. 4, pp. 1–32, 2024.

[43] G. Li, H. Zeng, H. Guo, Y. Ren, A. Dixon, Z. Cao, and T. Li, "Piezobud: A piezo-aided secure earbud with practical speaker authentication," in *Proceedings of ACM SenSys*, 2024.

[44] Z. Juncen, J. Cao, Y. Yang, W. Ren, and H. Han, "mmdrive: Fine-grained fatigue driving detection using mmwave radar," *ACM Trans. Internet Things*, vol. 4, no. 4, Nov. 2023.

[45] S. I. Siam, H. Ahn, L. Liu, S. Alam, H. Shen, Z. Cao, N. Shroff, B. Krishnamachari, M. Srivastava, and M. Zhang, "Artificial intelligence of things: A survey," *ACM Transactions on Sensor Networks*, 2024.

[46] Y. Ren, W. Sun, J. Du, H. Zeng, Y. Dong, M. Zhang, S. Chen, Y. Liu, T. Li, and Z. Cao, "Demeter: Reliable cross-soil lpwan with low-cost signal polarization alignment," in *Proceedings of ACM MobiCom*, 2024.

[47] J. Wang, X. Zhang, L. Xiao, and T. Li, "Survey for soil sensing with iot and traditional systems," *Network*, vol. 3, no. 4, pp. 482–501, 2023.

[48] J. Wang, Y. Feng, G. Kumbhar, G. Wang, Q. Yan, Q. Jin, R. C. Ferrier, J. Xiong, and T. Li, "Soilcares: Towards low-cost soil macronutrients and moisture monitoring using rf-vnir sensing," in *Proceedings of ACM MobiSys*, 2024.

[49] J. Bauer and N. Aschenbruck, "Towards a low-cost rssi-based crop monitoring," *ACM Trans. Internet Things*, vol. 1, no. 4, Jun. 2020.

[50] Y. Ren, L. Liu, C. Li, Z. Cao, and S. Chen, "Is lorawan really wide? fine-grained lora link-level measurement in an urban environment," in *Proceedings of IEEE ICNP*, 2022.

[51] Y. Ren, P. Cai, J. Jiang, J. Du, and Z. Cao, "Prism: High-throughput lora backscatter with non-linear chirps," in *Proceedings of IEEE INFOCOM*, 2022.

[52] J. Du, Y. Ren, Z. Zhu, C. Li, Z. Cao, Q. Ma, and Y. Liu, "Srlora: Neural-enhanced lora weak signal decoding with multi-gateway super resolution," in *Proceedings of ACM MobiHoc*, 2023.

[53] J. Du, Y. Liu, Y. Ren, L. Liu, and Z. Cao, "Loratrimmer: Optimal energy condensation with chirp trimming for lora weak signal decoding," in *Proceedings of ACM MobiCom*, 2024.

[54] J. Lin, R. Xiong, Z. Xu, W. Tian, C. Chen, X. Dong, and J. Luo, "Multi-node concurrent localization in lora networks: Optimizing accuracy and efficiency," in *Proceedings of IEEE INFOCOM*, 2024.

[55] Y. Ren, A. Gamage, L. Liu, M. Li, S. Chen, Y. Dong, and Z. Cao, "Sateriot: High-performance ground-space networking for rural iot," in *Proceedings of ACM MobiCom*, 2024.